Performance Analysis of ZigBeePRO Network Using the Shortest Path Algorithm for Distributed Renewable Generation

Syed Zahurul Islam[1, *], Mohammad Lutfi Othman[2], Syed Zahidul Islam[3]
[1]Power Integration System, Faculty of Electrical & Electronic Engineering,
Universiti Tun Hussein Onn Malaysia (UTHM),
Parit Raja, Johor, Malaysia
[2]Advanced Lightning, Power & Energy Research (ALPER),
Department of Electrical and Electronics Engineering, Faculty of Engineering,
Universiti Putra Malaysia (UPM),
Serdang, Selangor, Malaysia
[3]Radiation Solutions Inc.,
5875 Whittle Rd, Mississauga, ON, Canada
zahurul@uthm.edu.my

***Abstract*—The communication requirement for integrating Distributed Renewable Generation (DRG) into Smart Grid (SG) is not strict, where the reliability and critical demand of data delivery are compromised due to the low-data rate and power of ZigBee. However, the presence of various dielectric constant materials in the DRG can cause transmission impairments of the electromagnetic wave. In this paper, we have analysed the performance of the ZigBeePRO network by applying the shortest path algorithm while delivering energy data from the solar DRG to the SG. The DRG architecture is created by considering a real test-bed of 35 kW solar DRG at Universiti Putra Malaysia (UPM). The numbers of nodes are calculated from specifications of the ZigBeePRO enabled Waspmote embedded board, inverters, and electrical parameters of a Photovoltaic (PV) module. The results of the obtained propagation path loss model indicate that the Transverse Electric (TE) and Transverse Magnetic (TM) polarizations are proportional to the loss of the propagation path at different incident angles (α); however, an exception is observed for the TM polarization at α = 55 º. Due to this polarization effect, the brick-built type cabin at the DRG site is a consequence of a higher propagation path loss than the Iron (III)-made cabin. The other performance parameters, including network throughput, data loss, and ZigBeePRO collision, are also evaluated.**

***Index Terms*—Distributed renewable generation; Received signal strength indicator; Shortest path algorithm; ZigBeePRO.**

I. INTRODUCTION

The Smart Grid (SG) concept was first established approximately forty years ago due to many shortcomings arising in the existing exhausted power grid system, such as a slower and critical response time [1], mandatory data delivery for demand and energy forecasting from distributed power plants [2], and carbon emission issues [3]. Many countries, including Malaysia, have set a milestone in integrating Distributed Renewable Generation (DRG) into SG through wireless data communication technologies [4]. For this integration, the IEEE802.15.4 supported ZigBeePRO has been widely proposed by the previous research authors in [4]–[7]. In this application, the ZigBeePRO technology offers ease and lower installation and operating cost. In contrast, it has limitations on interference and spectrum resources [8]. Despite these limitations, ZigBeePRO technology is more feasible and advantageous over the other wireless technologies from the analysis of the SG network structure by many researchers [1]–[3], [8]–[10]. This trend of using ZigBeePRO technology is the motivation for examining network performance in the DRG application of SG.

In this paper, a ZigBeePRO network scenario is divided into several DRG sites, located adjacent to each other. ZigBeePRO nodes are assumed to be randomly placed at the DRG site. The overall network architecture is constructed as a multi-hop tree fashion, from the distributed end to the SG control centre. In one of the DRG sites, the ZigBeePRO nodes are considered to be deployed with solar generation. The deployed node collects the energy data from the inverter and exports them to the control centre. For this export service, we applied greedy algorithm to find the shortest and strongest weighted path of the Received Signal Strength Indicator (RSSI). The algorithm has the advantage of less complexity, which can reduce the processing time of the node's microprocessor and thus save energy. The algorithm may lead to longer routes caused by the avoidance of obstacles that result in a longer delay. However, in the DRG application, the nodes are placed with a line of sight at a certain height from the inverter. Due to open areas in the solar farm, there is a mere chance for the ZigBeePRO signals to face obstacles by trees, PV modules, or other

Manuscript received 15 June, 2021; accepted 16 November, 2021.
This research was supported by the Research Management Center, Universiti Tun Hussein Onn Malaysia (UTHM) through Tier1 (vot H758) and by Geran Putra Berimpak, Universiti Putra Malaysia (UPM) under project code UPM/800-3/3/1/GPB/2019/9671700.

avoidance. In addition to this, the slight delay in the delivery of energy data from the DRG to the control centre is not crucial, based on the findings of our previous research [4]. The novelty of this study is that we have conducted a performance analysis on a range of ZigBeePRO networks, namely network throughput, packet loss, and collision under the DRG scenario, while the electromagnetic ZigBeePRO radio wave is included to investigate propagation loss through dielectric constant materials, transverse electric, and magnetic polarization effect analysis.

There are several recent researches related to ZigBee and network performance in different SG networks, such as substations, power control room, and transformer vault [10]. The performance parameters were end-to-end delay, throughput, packet delivery ratio, and energy consumption. Another practical experiment was conducted indoors for the performance evaluation of 51 ZigBee nodes in terms of transmission throughput, packet loss rate, and node connectivity [11]. Collisions were observed in star topology due to multi-hopping and setting lower value of the backoff exponent. A higher value of the backoff parameter decreases collisions, but it also decreases battery life [12]. Hanzalek and Jurcik presented a novel method to minimize the energy consumption of the ZigBee beacon enabled cluster tree network by setting a time division scheduling period [13]. In [14], the packet drop rate and end-to-end delay were analysed in another cluster tree based wireless sensor network using the proposed algorithm. In [15], energy efficiency is evaluated in broadcast and multicast environments by developing the broadcast incremental power algorithm.

Taking into account the PER performance metric, ZigBee was practically studied with other nearby Industrial, Scientific and Medical (ISM) bands using a home energy network test-bed [16]. In simulation based design for home area network using ZigBee, the direct spread spectrum, Offset Quadrature Phase-Shift Keying (OQPSK) modulation, non-coherent type of receiver are used to reduce the interference, complexity, and overall cost. The bit error rate and signal-to-noise ratio of the transceiver model are shown graphically, but the performance is not analysed [17]. In [18], the fast joining technique is proposed for a meter to join a ZigBee coordinator in the advanced metering infrastructure by eliminating the scanning time. The technique improves the node joining time up to 500 m distance, however, Zigbee interference with WiFi was not considered in the analysis. The other algorithm proposed for a short joining time for ZigBee in different topologies, such as the fast association mechanism for the star topology [19], the fast association process for the tree topology [20], and the scheduling algorithm for the beacon collision problem in the tree topology [21].

In [22], the propagation path loss was obtained in free space, simulation, and from measured data at three different frequencies other than the 2400 MHz frequency. The inclusion of the height of the tree trunk in the piecewise model is the significance of the research. The model shows 18 % to 30 % less error than other models compared in that analysis. The path loss was analysed from experimental data in the concrete school building and parking lot environment inside a shopping mall by the authors in [23] and the forest environment (palm tree plantation in Singapore) - by the authors in [24]. In [23], the ceiling and antenna height can affect the breakpoint distance characteristics at the mobile band frequency. The proposed model estimated the path loss in the indoor environment and showed performance up to a distance of 1.2 km. On the other hand, the authors in [24] proposed the ITU-R model in the Ultra High Frequency (UHF) and Very High Frequency (VHF) bands and experimented at different frequencies. Improvement of the model can solve the lateral wave problem in the VHF band.

In addition to ZigBee, another 2.4 GHz operating technology called “Wi-Fi” was considered for protecting the power system in a critical time condition [25]. The authors considered this technology for model analysis and for the benchmark performance of the wireless network in SG. This technology was also proposed for an automatic meter reading and a new mesh-type routing algorithm [26].

None of these works has studied the performance of the ZigBeePRO network in the DRG environment. Therefore, different from the discussed related reviews, it is attempted to deploy the shortest path algorithm and analyse the ZigBeePRO network considering a real-world DRG environment by providing related mathematical models in the concept of integrating DRG with the SG. The contribution of this research can be summarized in three ways:

– The RSSI based shortest path algorithm is applied for the energy data import service using ZigBeePRO communication by considering a real test-bed, 35 kW solar power plant at Universiti Putra Malaysia (UPM);

– Different properties of the solar DRG site, such as antenna placement and uneven presence of obstacles, are investigated for the performance analysis of the ZigBeePRO network, namely network throughput, packet loss, and collision;

– Due to the presence of these properties, the Electromagnetic ZigBeePRO wave effect can cause transmission impairment which is considered by analysing dielectric constant materials, transverse electric, and magnetic polarizations.

The approach proposed by the latest ZigBeePRO protocol is better than the existing technology because it is convenient for sensor integration over the other communication technologies. In addition, it supports longer coverage, low power consumption, a large number of child node integration, and better data encryption over Wi-Fi. Therefore, in this research, the critical issues of the DRG environment and the network performance of the ZigBeePRO are considered for modeling and evaluation.

II. ZIGBEE COMMUNICATION ARCHITECTURE FOR DRG

Figure 1 is illustrated to explain the connectivity of the network considering a real test-bed of solar DRG at the Universiti Putra Malaysia (UPM), location coordinate 22.945 ° North and 101.75 ° East. The 10 kW solar DRG is planned to extend up to 35 kW, which we consider as DRG integration into the SG using the ZigBeePRO network. In the network, we consider three sites, namely DRG site 1, site 2, and site 3. The DRG site 2 and site 3 consist of a BIPV/FiT network, where the DRG site 1 is dedicated for a

35 kW large solar DRG. The overall architecture of the network is a tree topology - from distributed end point to the control centre via mesh routers (Fig. 1(a)). Mesh routers, such as Gateway G2, Gateway G3, and Gateway G4, are served as Personal Area Network (PAN) coordinators of DRG site 2, DRG site 1, and DRG site 3, respectively. All routers are interlinked with each other through Wi-Fi mesh communication coordinated by Gateway G1 (Fig. 1(b)). A separate network from gateway G1 is created to connect it to the control centre. Depending on the geographical location of Gateway G1 and the control centre, any of the communication technologies (4G/5G/Wi-Fi/optical) can be considered for this network. For example, if the location of Gateway G1 is in a remote territory and there is no coverage with any nearby Wi-Fi mesh network, Gateway G1 can be connected solely to the control centre through 4G/5G or optical fibre communication.

The RSSI based shortest path algorithm is applied in the DRG site 3 - a mesh network consists of a large number of nodes. The nodes are referred to as sensors with the integrated ZigBeePRO embedded board. All the nodes act as a Fully Functional Device (FFD) and one of them coordinates the mesh network. In practice, each smart inverter is an FFD, because the FFDs are integrated into it. A separate FFD can be used for environmental data record, installed at the DRG substation. According to the modern specification of the smart solar inverter, nodes are connected to the inverter where the ZigBeePRO radio can be placed at a height of 3.5 m (including structural height) from the roof of the inverter with a line of sight. Therefore, the number of FFDs depends on the number of inverters required, which is determined from the DRG capacity. An extensive discussion on the DRG mesh network and the practical use of the ZigBeePRO coalesced FFD for monitoring energy data under a solar DRG can be found in our previous researches in [4] and [27], respectively.

In the proposed approach, all nodes are assumed to be FFDs under the DRG mesh network. This is because the integration of the DRG into the SG control centre is a two-way data communication technology [4], and each ZigBeePRO node performs a two-way data communication service. The network can be used to control distributed nodes from the control centre without physical access. In addition, when the ZigBeePRO at the DRG serves for data monitoring, it will be required to upgrade, program modify, insert new-task, and other jobs. However, consider all the nodes, as FFDs can increase the power consumption. Based on our research, the increase is insignificant because the frequency of data delivery in this application is low, generally 3 samples/min is sufficient [27].

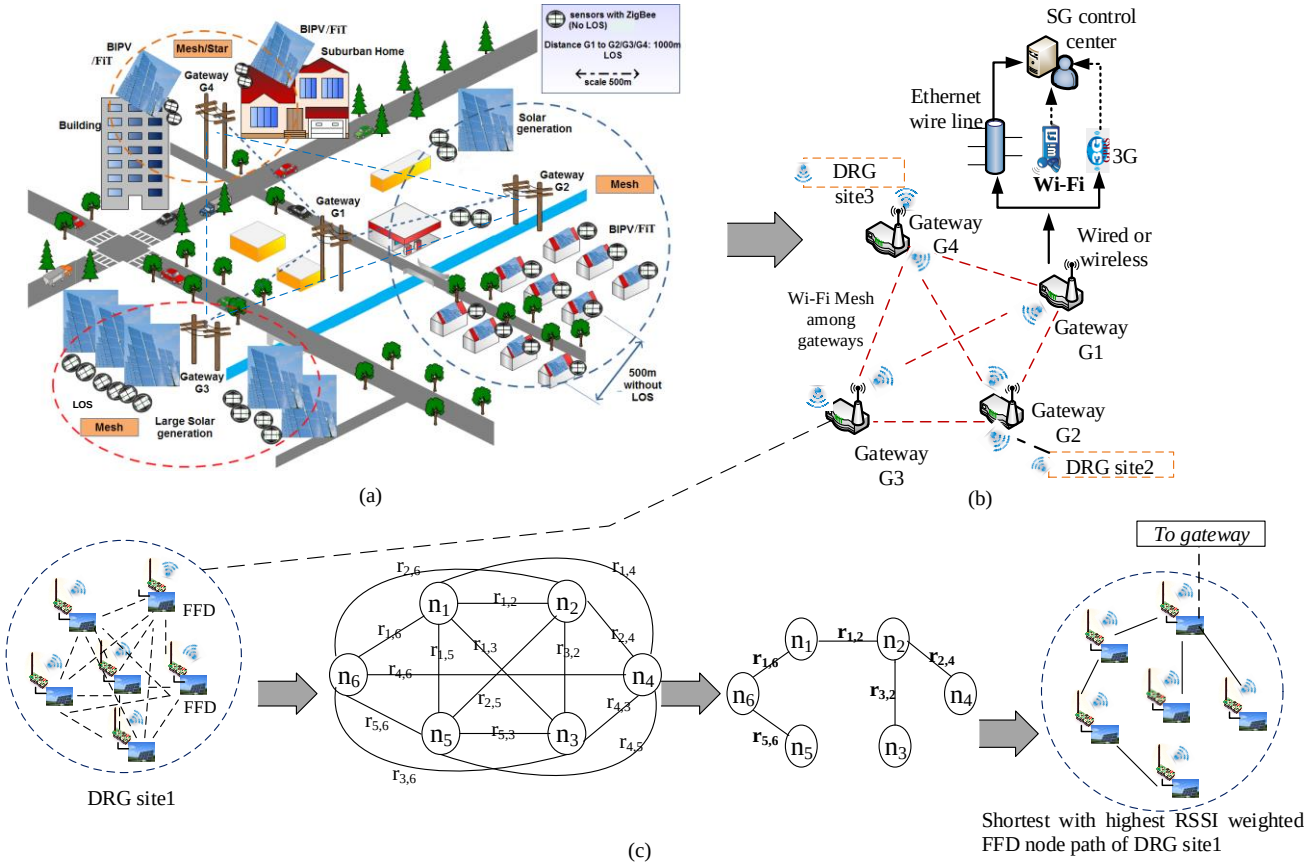

Fig. 1. (a) Wireless communication architecture to integrate DRG with SG; (b) Each DRG site has one ZigBeePRO network where multiple FFD nodes form the network; (c) The shortest and highest RSSI weighted path obtained.

III. PROPOSED SHORTEST PATH ALGORITHM FOR DRG

Nodes are operated following a greedy Prim's algorithm. The greedy choice finds the minimum shortage path for forwarding the data to the PAN coordinator. To implement the algorithm, a graph is assumed to consist of nodes where G and I are the set of nodes and the set of nodes' interconnections, respectively. Then $G \equiv \{n_1, n_2, \ldots\ldots, n_k\}$, where $k \in Z$, and each of the interconnections denotes as $r_{i,j} \in I$. In addition, for each $i(1 \le i \le k)$, there is a j such that $j = j+1 \; and \; 0 \le j < k$. If k is a total number of nodes

at G, I will consist of $\frac{k(k-1)}{2}$ number of edges at most.

It is also assumed that every node $n_i \in G$ of a network acts as a FFD. It means that each of $\{n_1, n_2, \ldots, n_k\}$ FFD node can perform as both operational node and network coordinator. Among these coordinators, only one is the central PAN coordinator denoted by n_c. The n_c has extra computational capabilities over any $G-\{n_c\}$ FFD node of the network. There are also algorithms for electing n_c and techniques to overcome the attempt of multiple coordinators to become a central PAN coordinator [28]. After the election of n_c, it sends a broadcast message. Upon receiving the broadcast message, the $G-\{n_c\}$ numbers of FFDs also send Acknowledgements (ACKs) in broadcast mode. If every n_i sends one ACK, the total $(k-1)$ number of ACK messages will be broadcasted, and each n_i will receive at most $(k-2)$ numbers of ACK messages (2 nodes are excluded: n_c and itself). On the basis of the received ACKs, each n_i can estimate the corresponding RSSI ($r_{i,j}$) and also the distances ($d_{i,j}$) of its neighbor FFDs. Many previous researchers have modeled RSSI as a function of the distance between the sender node and the receiver node (1) [29]. The RSSI value is considered as a weight of the interconnection between the sender FFD and the receiver FFD; e.g., the weight of the RSSI value of (n_i, n_j) or (n_j, n_i) is $r_{i,j}$ or $r_{j,i}$. As both FFDs are symmetrical and bidirectional, it can be written $r_{i,j} = r_{j,i}$ and $d_{i,j} = d_{j,i}$

$$r_{1,1}, r_{1,2}, \ldots\ldots r_{i,j} = -10\tau \log[d_{1,1}, d_{1,2}, \ldots\ldots d_{i,j}] + \psi, \quad (1)$$

where τ and ψ are the path loss exponent and constant, respectively. Following the above-mentioned procedure, a connected and undirected weighted graph is formed analytically. Now, the objective is to construct a path (T) that spans the weighted graph such that T must be acyclic with a weight of $r_{i,j}$ and $T \subseteq I$. Then the total weight will be maximized when (2) is true

$$r_{i,j}(T) = Max[\sum r_{i,j}(n_i, n_j)], \quad (2)$$

provided $(n_i, n_j) \in T$.

Therefore, in particular, two conditions must be ensured while building up T. First, it should not be cyclic, which means another technique is required for choosing appropriate weighted path so that the forming graph always remains undirected. Second, at every iteration during building up T, the value of the weighted graph must be the maximum among all possible trees.

To build up T from the graph, it is possible to determine the weight of (n_i, n_j) at each iteration and append it to a set called "P". However, the condition of appending this weight of (n_i, n_j) is - P must be a proper subset of T (i.e., $P \subseteq T$) and the weight of (n_i, n_j) exists such that $(n_i, n_j) \in T, (n_i, n_j) \notin P$. By ensuring this condition, the maximum weighted base path can be determined for forwarding data from each node to the PAN coordinator through the shortest unidirectional way. The algorithm is explained in more detail as the following steps:

– *Step 1*. First, M is considered as k×k matrix that determines the weight of the graph. M is defined as $r_{i,j} = r_{j,i} =$ the weight of the edge (n_i, n_j) when n_i and n_j are neighbors; $r_{i,j} = r_{j,i} = \infty$ when n_i and n_j are not neighbors, and $r_{i,i} = \infty$.

All positive weights in M are converted to negative because the values of RSSI are negative (according to (1)). Therefore, from now on, the determination of the minimum values weighted path is explained in the following steps.

The first FFD node n_1 is connected to n_p, where n_p is the closestto node n_1 (n_p is closest to n_1 if $n_1 n_p$ (i.e., $r_{1,p}$) is an interconnection with minimum possible weight). Node n_p can be obtained from matrix M. In fact, node n_p corresponds to the entry in row 1 of M, which is minimum.

– *Step 2*. Having chosen n_p, consider that $n_i \neq n_1$ or n_p is a node corresponding to the smallest entry in rows 1 and p together. Then node n_i is the sub-graph stated by weight $n_1 n_p$ (i.e., $r_{1,p}$). n_i is connected to n_1 or n_p, according to whether the entry is in row 1 or p^{th} row. If it is in the p^{th} row, it is the $(p, i)^{th}$ entry of M.

– *Step 3*. The sub-graph is considered and can be defined by a weight set $\{n_1 n_p, n_p n_i\}$ or $\{r_{1,p}, r_{p,i}\}$. Then the set of nodes of the closest neighbors is determined like $\{n_1, n_p, n_i\}$.

– *Step 4*. The process is continued until all the n_i nodes are connected by $(k-1)$ number of interconnections.

Taking into account Fig. 1(b), M is formulated from the DRG site. -1 scalar value is multiplied by M to change all the RSSI values into positive, since RSSI denoted as $-dBm$ indicates the signal level of the last good packet received (i.e., $-40\,dBm$ RSSI is a higher signal strength than $-80\,dBm$). Therefore, finding the smallest value in M basically denotes the highest RSSI valued path of the network (3)

$$M = \begin{array}{c} \\ n_1 \\ n_2 \\ n_3 \\ n_4 \\ n_5 \\ n_6 \end{array} \begin{array}{c} \begin{array}{cccccc} n_1 & n_2 & n_3 & n_4 & n_5 & n_6 \end{array} \\ \begin{bmatrix} \infty & r_{1,2} & r_{1,3} & r_{1,4} & r_{1,5} & r_{1,6} \\ r_{2,1} & \infty & r_{2,3} & r_{2,4} & r_{2,5} & r_{2,6} \\ r_{3,1} & r_{3,2} & \infty & r_{3,4} & r_{3,5} & r_{3,6} \\ r_{4,1} & r_{4,2} & r_{4,3} & \infty & r_{4,5} & r_{4,6} \\ r_{5,1} & r_{5,2} & r_{5,3} & r_{5,4} & \infty & r_{5,6} \\ r_{6,1} & r_{6,2} & r_{6,3} & r_{6,4} & r_{6,5} & \infty \end{bmatrix} \end{array}. \quad (3)$$

In the row n_1 node, it is assumed that $r_{1,2}$ is the smallest weight that is under column n_2. So, the path of n_1 and n_2 nodes is created with the weight value $r_{1,2}$. In the next step, columns n_1 and n_2 are neglected (since they are joined already); however, consider their rows put together, e.g., $\begin{cases} r_{1,2} & r_{1,4} & r_{1,5} & r_{1,6} \\ r_{2,3} & r_{2,4} & r_{2,5} & r_{2,6} \end{cases}$, the smallest weight is obtained denoted by $r_{2,3}$. Since it occurred in column n_3 and row n_2, the path n_2 is extended towards n_3 with the weight value $r_{2,3}$. Next, like in the previous step and excluding three columns

of n_1, n_2, and n_3, but putting their rows together, $r_{1,5}$ (assume) is the smallest. It leads to n_5 connecting to n_1. Continuing likewise, finally, the shortest with highest RSSI weighted path can be obtained as in Fig. 1(c).

IV. Simulation Results and Analysis

In the simulation, the 35 kW capacity of the solar DRG and its surroundings at UPM are considered. First, we have identified the number of FFD nodes required from the solar DRG capacity. Prior to that, we formulate the FFD node considering Libelium manufactured Waspmote embedded board, which contains 7 analog inputs. Therefore, the board can measure 7 electrical parameters, namely open circuit voltage, short circuit current, maximum voltage, maximum current, AC current, AC voltage, and PV module temperature. A board with the ZigBeePRO (an FFD) can be used for one inverter, suitable to support 1 kW capacity of PV. Since the DRG is 35 kW, there are 35 FFDs required taking into account the 1 FFD/1 kW inverter. The ZigBeePRO radio is installed at a height of 3.5 m from the roof of the inverter. In Fig. 2(a), the Google map image of the 10 kW solar DRG site is shown, an open place located at UPM. A banquet hall is around 300 m from the site, potential for FiT (currently it is called "net energy metering" or "NEM") implementation. A wind turbine is also located near the DRG site but is not hybrid with the solar. Around 500 m from the site is the Chancellor building, considered another potential place for the NEM project. The real scenario of the three sites resembles the overall DRG architecture, explained in Fig. 1. In Fig. 2(b), the simulation layout of 35 FFDs, the centre PAN of the solar DRG, and the surrounding environment are shown. The arrow direction generated by the simulator shows the shortest and strongest RSSI based data path based on the model explained in Fig. 1 as DRG site 1.

The parameters of the simulation conducted in NCTUns are categorized as antenna properties, signal path loss properties, and uneven presence of obstacles (Table I).

The antenna height and gain values are from the Libelium manufactured ZigBeePRO (Table I). The environmental scenario and the related parameters are set according to the UPM solar DRG (uneven presence of obstacles), situated in an open place. Due to the existence of nearby streets and buildings, we set values for the signal path loss properties. To achieve realistic results, the open source simulator NCTUns is found to be one of the suitable tools for the traffic generation, maintaining the ZigBeePRO standard, and its protocol values. The simulator provides convenient Graphical User Interface (GUI) features with real life application program, which can be configured according to the test-bed of the solar DRG at UPM.

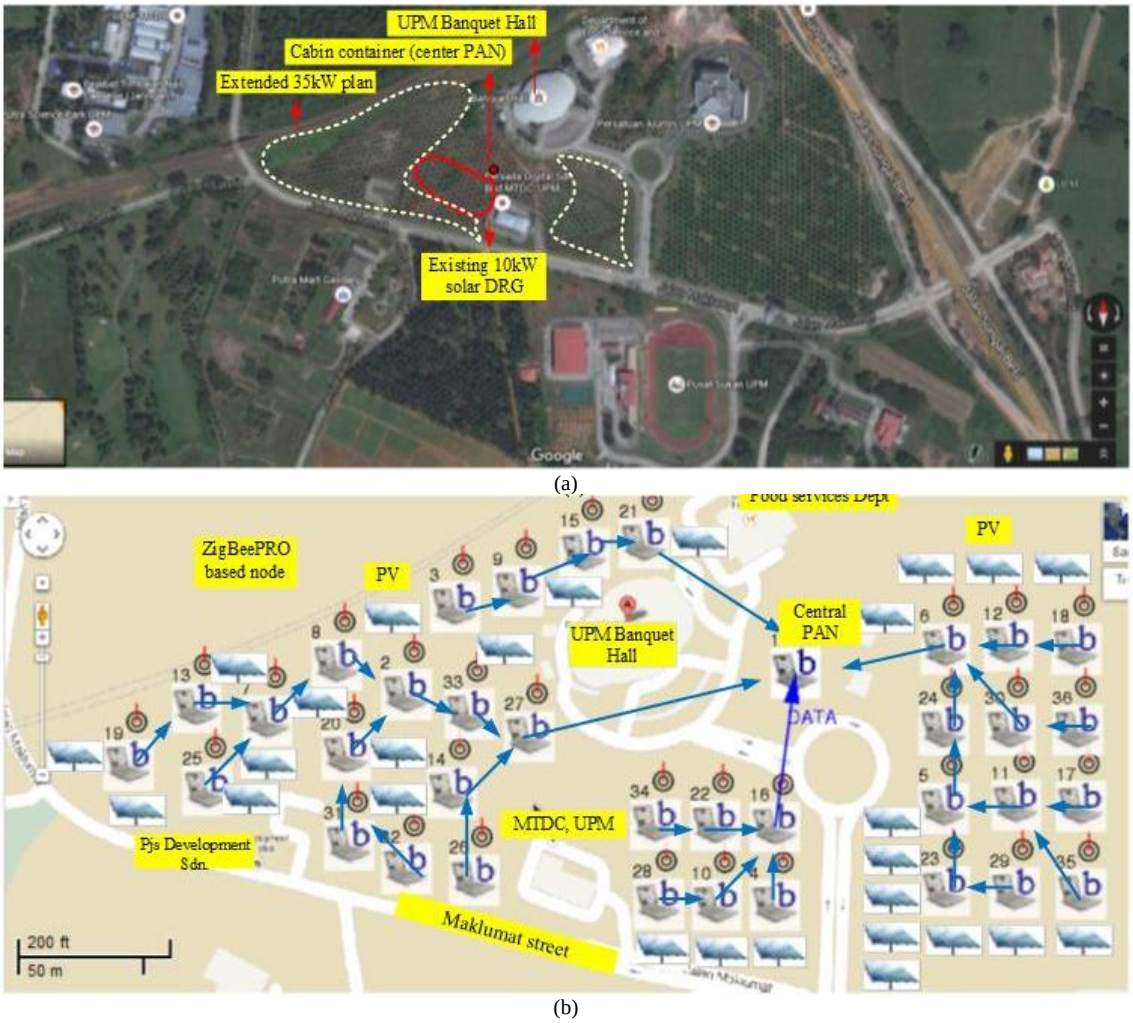

Fig. 2. The 35 kW DRG simulation scenario in NCTUns: (a) Location coordinate 22.945 ^{0} North 101.75 ^{0} East, obtained from Google map; (b) Direction shows the shortest and strongest RSSI based data path based on the model explained in Fig. 1. Central PAN coordinator (n_c) is marked as node1.

TABLE I. PARAMETERS AND RESPECTIVE VALUES FOR SIMULATION CONDUCTED IN NCTUns.

Parameters	Value
Antenna properties	
Height	3.5 m
Beam-width	360 ^{0}
Pointing direction	90 ^{0}
Gain	3
Signal path loss properties	
Model	Free space and shadowing
Exponent	2.2
Uneven presence of obstacles	
Average building height	10 m
Nearby Street width	3 m
Average building distance	100 m
Standard deviation	2
Node transmission power	30 dBm

A. Network Throughput Analysis

Figure 3 shows the throughput comparison between the shortest path algorithm and the star topology. It shows that the throughput of the network of the shortest path algorithm is higher than that of the star topology (Fig. 3(a)). A similar scenario is seen when the throughput of any random node is obtained (Fig. 3(b)).

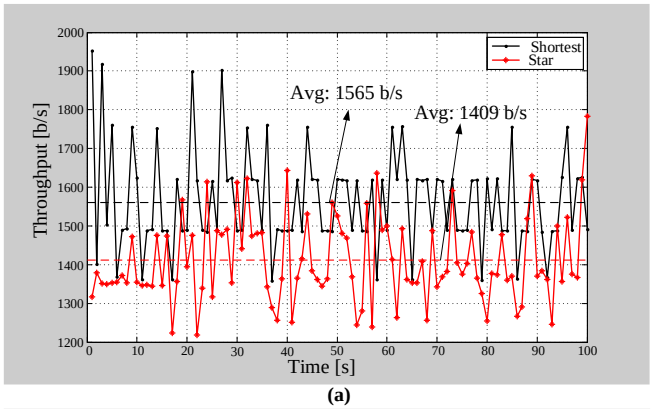

Fig. 3. Throughput analysis between the shortest path and star topology at 35 kW solar DRG environment when: (a) overall network throughput, (b) random node throughput. Mean throughputs are shown using dashed lines.

The reason for achieving a better throughput is that the packets produced by multiple nodes in star topology are waiting in the packet buffer queue, whereas there are other available paths for the packet forwarding to the destination in the shortest path algorithm. The mean throughput obtained is 1409 b/s (star) and 1565 b/s (shortest path). Our results are supported by [10] and [30] where the throughput of a ZigBee network achieved was 1077 b/s and 15933 b/s from the experimental work. A simulation was conducted considering 20, 40, and 60 nodes in star, mesh, and cluster tree topologies, which show the throughput in the range of 20 Kb/s–160 Kb/s [11]. Another research obtained a throughput of 1178 b/s for the 50 node scenario in cluster tree topology using QualNet simulation work [31]. Our simulation result is similar to that of previous researchers; however, a mere variation is observed due to different environment and communication setup, such as placement height of the receiver antenna, two-hop communication, number of nodes, and type of power supply for the nodes.

B. Packet Loss Rate and Collision Analysis

A collision in the shortest path algorithm is achieved lower than the star topology as depicted in the overlay bar diagram (Fig. 4). The collision is monitored at every 5 s taking into account the average number of collision packets. The initial collision (at the first instant) is approximately 75 % higher in both algorithms compared to the following instances. This is because multiple nodes intend to send packets simultaneously at the beginning, and the frames get despoiled. Later on, there became fewer collisions, and the performance of both algorithms improved.

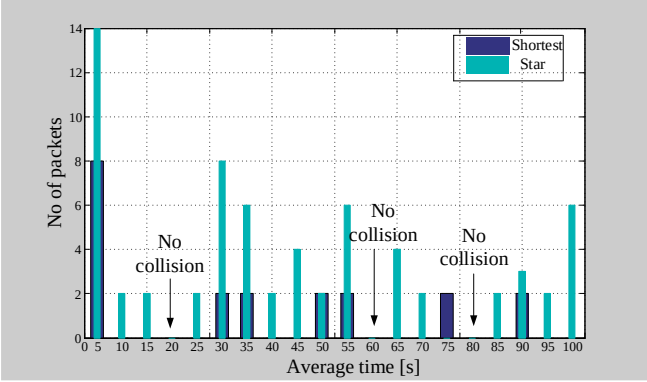

Fig. 4. Collision of network.

The stacked bar in Fig. 5 shows the packet loss rate over the 100 s simulation time. Like in a collision scenario, the packet loss rate is initially high and decreases over time (2 % for a star and 1.5 % for the shortest path). The average loss rates of the shortest path and star topology are 0.4967 % and 0.65 %, respectively. This inconsistent rate scenario has also been observed by previous researchers, where the loss rate is between 0.0 % and 6.0 % [10], [11], [32]. Our loss rate obtained is lower than the results of previous researchers because the nodes generate periodic packets consistently in our simulation. The comparison of the packet loss rate in Table II shows better performance of the shortest path algorithm.

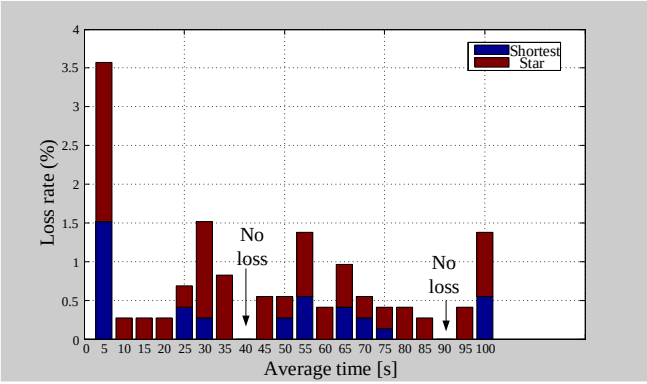

Fig. 5. Average packet loss rate as a function of time.

TABLE II. COMPARISON ANALYSIS FOR PACKET LOSS RATE.

Methods/Experiment	Maximum (%)	Minimum (%)	Average (%)
Silva *et al.* [10]	4	0	0.3
Arora, Sharma, and Sachdeva [11]	6.7	0	-
F. Ding and A. Song [32]	6.0	0	3.0
Star	2.1	0	0.65
Shortest path	1.5	0	0.4967

C. TM and TE Polarization Analysis

The reflection coefficients for Transverse Electric (TE) and Transverse Magnetic (TM) polarization are analysed based on the model explained in [33] in the aspect of Iron III oxide red made unpainted container cabin placed at UPM solar DRG. Figure 6 illustrates that the reflected power (dB) is a function of incident angle (α) for TE and TM polarization. It shows that when α increases, the reflected power of TE polarization also increases. However, the opposite scenario is observed for TM polarization until $\alpha = 55°$ and no reflection occurs at this incident angle.

Figure 7 shows that the reflection power increases with the increase of the dielectric constant for any incident angle except for TM polarization. For the dielectric constant from 1.5 to 3.5, the rate of the reflected power for both polarizations is higher than for the onward dielectric constants. Based on this characteristic, instead of brick or concrete based wall, the Iron III made container cabin is chosen for installing a receiver at the DRG site. This choice can decrease the overall loss in wave propagation.

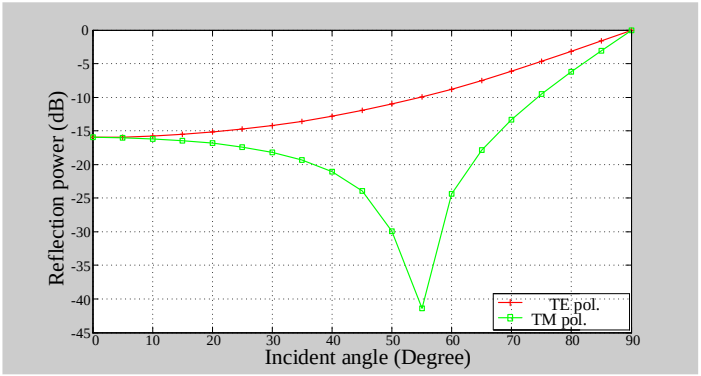

Fig. 6. TE and TM polarization effect for Iron III, dielectric constant, 1.9 with variable incident angles ($\alpha = 0° - 90°$). Pol. refers to polarization.

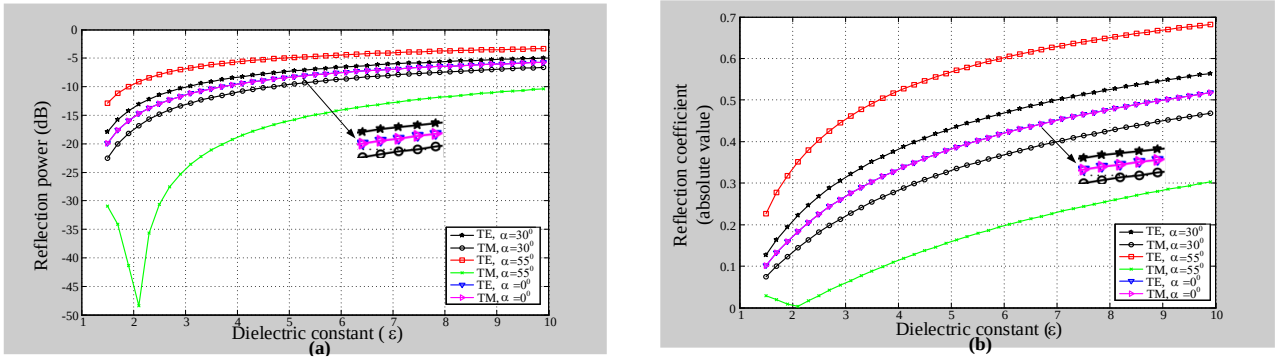

Fig. 7. (a) Reflected power in logarithm scale; (b) Reflection coefficient in absolute value - for Iron III, where incident angle is a function of the dielectric constant. $\alpha = 0°$ (direct wave propagation) shows the symmetrical characteristic for both TE and TM polarization.

V. CONCLUSIONS AND FUTURE DIRECTION

The main goal is to analyse the ZigBeePRO wireless network in the DRG environment, ensuring data delivery from the DRG solar site to the SG control centre. To achieve the goal, this paper has undertaken to model the shortest and strongest RSSI weighted path algorithm for the ZigBeePRO network. It is attempted to analyse the network performance considering the complexity of the non-ideal DRG environment. Based on the evaluation of 35 kW solar DRG, the overall throughput of the star topology (1409 b/s) outperforms the shortest path algorithm (1565 b/s). On the other hand, both the star and the shortest path methods show 75 % higher packet collisions at the initial instant compared to the subsequent simulation time. This trend is also observed in the case of the packet loss rate, while the average loss rate of star and shortest methods is 0.65 % and 0.497 %, respectively. The analysis of TE and TM polarization and the results of the dielectric constant from 1.5 to 3.5 suggest using an iron made cabin in the DRG environment as a brick-built cabin can cause a higher propagation path loss.

Although the simulation results on the network parameters do not confirm the exact performance of the ZigBeePRO in the DRG environment, it does partially substantiate that the integration of the DRG into the SG is manageable by applying the shortest path algorithm in the ZigBeePRO network. More research is needed to obtain the actual path loss by determining the path loss exponent, the ideal path gain, and the zero-mean Gaussian variable from the experimental work. The parameters and mathematical model investigated in this work for the ZigBeePRO protocol will support the future experimental work in this special domain of the SG.

ACKNOWLEDGMENT

The authors would like to thank Wong Chai Jen for assisting with her support to format this paper. We also

appreciate Hashim Hizam, Noor Izzri Abdul Wahab, and Peter Crossley for their advice and valuable comments in this research work.

CONFLICTS OF INTEREST

The authors declare that they have no conflicts of interest.

REFERENCES

[1] D. Bian, M. Kuzlu, M. Pipattanasomporn, S. Rahman, and D. Shi, "Performance evaluation of communication technologies and network structure for smart grid applications", *IET Communications*, vol. 13, no. 8, pp. 1025–1033, 2019. DOI: 10.1049/iet-com.2018.5408.

[2] X. Huang, J. Shi, B. Gao, Y. Tai, Z. Chen, and J. Zhang, "Forecasting hourly solar irradiance using hybrid wavelet transformation and elman model in smart grid", *IEEE Access*, vol. 7, pp. 139909–139923, 2019. DOI: 10.1109/ACCESS.2019.2943886.

[3] Y. Cheng, N. Zhang, Y. Wang, J. Yang, C. Kang, and Q. Xia, "Modeling carbon emission flow in multiple energy systems", *IEEE Transactions on Smart Grid*, vol. 10, no. 4, pp. 3562–3574, 2019. DOI: 10.1109/TSG.2018.2830775.

[4] S. Zahurul, N. Mariun, I. V. Grozescu, H. Tsuyoshi, Y. Mitani, M. L. Othman, H. Hizam, and I. Z. Abidin, "Future strategic plan analysis for integrating distributed renewable generation to smart grid through wireless sensor network: Malaysia prospect", *Renewable and Sustainable Energy Reviews*, vol. 53, pp. 978–992, 2016. DOI: 10.1016/j.rser.2015.09.020.

[5] S. Zahurul, N. Mariun, I. V. Grozescu, M. Lutfia, H. Hashima, and M. Amrana, Izham, "Development of a prototype for remote current measurements of PV panel using WSN", *International Journal of Smart Grid and Clean Energy*, vol. 3, no. 2, pp. 241–246, 2014. DOI: 10.12720/sgce.3.2.241-246.

[6] S. Zahurul, N. Mariun, M. L. Othman, H. Hizam, I. Z. Abidin, and A. Toudeshki, "Ambient temperature effect on amorphous silicon (a-si) photovoltaic module using sensing technology", in *Proc. of 2015 9th International Conference on Sensing Technology (ICST)*, 2015, pp. 235–241. DOI: 10.1109/ICSensT.2015.7438399.

[7] S. Zahurul, N. Mariun, L. Kah, H. Hizam, M. L. Othman, I. Z. Abidin, and Y. Norman, "A novel zigbee-based data acquisition system for distributed photovoltaic generation in smart grid", in *Proc. of 2015 IEEE Innovative Smart Grid Technologies-Asia (ISGT ASIA)*, 2015, pp. 1–6. DOI: 10.1109/ISGT-Asia.2015.7387097.

[8] M. A. Setiawan, F. Shahnia, S. Rajakaruna, and A. Ghosh, "Zigbee based communication system for data transfer within future microgrids", *IEEE Transactions on Smart Grid*, vol. 6, no. 5, pp. 2343–2355, 2015. DOI: 10.1109/TSG.2015.2402678.

[9] V. C. Gungor, B. Lu, and G. P. Hancke, "Opportunities and challenges of wireless sensor networks in smart grid", *IEEE Transactions on Industrial Electronics*, vol. 57, no. 10, pp. 3557–3564, 2010. DOI: 10.1109/TIE.2009.2039455.

[10] M. R. Silva, E. S. Souza, P. J. Alsina, D. L. Leite, M. R. Morais, D. S. Pereira, L. B. P. Nascimento *et al.*, "Performance evaluation of multi-UAV network applied to scanning rocket impact area", *Sensors*, vol. 19, no. 22, p. 4895, 2019. DOI: 10.3390/s19224895.

[11] V. K. Arora, V. Sharma, and M. Sachdeva, "On QoS evaluation for ZigBee incorporated Wireless Sensor Network (IEEE 802.15. 4) using mobile sensor nodes", to be published in *Journal of King Saud University-Computer and Information Sciences*. DOI: 10.1016/j.jksuci.2018.10.013.

[12] M. Fruth, "Formal methods for the analysis of wireless network protocols", Ph.D. dissertation, Oxford University, 2011.

[13] Z. Hanzalek and P. Jurcik, "Energy efficient scheduling for cluster-tree wireless sensor networks with time-bounded data flows: Application to IEEE 802.15. 4/Zigbee", *IEEE Transactions on Industrial Informatics*, vol. 6, no. 3, pp. 438–450, 2010. DOI: 10.1109/TII.2010.2050144.

[14] W.-J. Liu, D. Zhao, and G. Zhu, "End-to-end delay and packet drop rate performance for a wireless sensor network with a cluster-tree topology", *Wireless Communications and Mobile Computing*, vol. 14, no. 7, pp. 729–744, 2014. DOI: 10.1002/wcm.2230.

[15] J. E. Wieselthier, G. D. Nguyen, and A. Ephremides, "On the construction of energy-efficient broadcast and multicast trees in wireless networks", in *Proc. of IEEE INFOCOM 2000. Conference on Computer Communications. Nineteenth Annual Joint Conference of the IEEE Computer and Communications Societies (Cat. No. 00CH37064)*, 2000, pp. 585–594, vol. 2. DOI: 10.1109/INFCOM.2000.832232.

[16] M. A. Sarijari, M. S. Abdullah, A. Lo, and R. A. Rashid, "Experimental studies of the zigbee frequency agility mechanism in home area networks", in *Proc. of 39th Annual IEEE Conference on Local Computer Networks Workshops*, 2014, pp. 711–717. DOI: 10.1109/LCNW.2014.6927725.

[17] G. S. Beula and P. Rathika, "Zigbee transceiver design for smart grid home area network using Matlab Simulink", in *Proc. of 2020 International Conference on Emerging Trends in Information Technology and Engineering (ic-ETITE)*, 2020, pp. 1–5. DOI: 10.1109/ic-ETITE47903.2020.311.

[18] C.-H. Ke, S.-Y. Hsieh, T.-C. Lin, and T.-H. Ho, "Efficiency network construction of advanced metering infrastructure using Zigbee", *IEEE Transactions on Mobile Computing*, vol. 18, no. 4, pp. 801–813, 2019. DOI: 10.1109/TMC.2018.2848237.

[19] F. Meng and Y. Han, "A new association scheme of IEEE 802.15. 4 for real-time applications", in *Proc. of 2009 5th International Conference on Wireless Communications, Networking and Mobile Computing*, 2009, pp. 1–5. DOI: 10.1109/WICOM.2009.5301369.

[20] M. Javed, K. Zen, H. B. Lenando, and H. Zen, "Fast Association Process (FAP) of beacon enabled for IEEE 802.15. 4 in strong mobility", in *Proc. of 2013 8th International Conference on Information Technology in Asia (CITA)*, 2013, pp. 1–8. DOI: 10.1109/CITA.2013.6637555.

[21] L.-H. Yen, Y. W. Law, and M. Palaniswami, "Risk-aware distributed beacon scheduling for tree-based Zigbee wireless networks", *IEEE Transactions on Mobile Computing*, vol. 11, no. 4, pp. 692–703, 2012. DOI: 10.1109/TMC.2011.88.

[22] O. Kurnaz and S. Helhel, "Near ground propagation model for pine tree forest environment", *AEU-International Journal of Electronics and Communications*, vol. 68, no. 10, pp. 944–950, 2014. DOI: 10.1016/j.aeue.2014.04.019.

[23] S. Phaiboon, P. Phokharatkul, and S. Somkuarnpanit, "New upper and lower bounds line of sight path loss model for mobile propagation in buildings", *AEU-International Journal of Electronics and Communications*, vol. 62, no. 3, pp. 207–215, 2008. DOI: 10.1016/j.aeue.2007.03.021.

[24] Y. S. Meng, Y. H. Lee, and B. C. Ng, "Empirical near ground path loss modeling in a forest at VHF and UHF bands", *IEEE Transactions on Antennas and Propagation*, vol. 57, no. 5, pp. 1461–1468, 2009. DOI: 10.1109/TAP.2009.2016703.

[25] Y. Xu and W. Wang, "Wireless mesh network in smart grid: Modeling and analysis for time critical communications", *IEEE Transactions on Wireless Communications*, vol. 12, no. 7, pp. 3360–3371, 2013. DOI: 10.1109/TWC.2013.061713.121545.

[26] L. Li, X. Hu, and B. Zhang, "A routing algorithm for WiFi-based wireless sensor network and the application in automatic meter reading", *Mathematical Problems in Engineering*, vol. 2013, 2013. DOI: 10.1155/2013/320894.

[27] S. Z. Islam, M. L. Othman, M. Saufi, R. Omar, A. Toudeshki, and S. Z. Islam, "Photovoltaic modules evaluation and dry-season energy yield prediction model for NEM in Malaysia", *PLoS One*, vol. 15, no. 11, p. e0241927, 2020. DOI: 10.1371/journal.pone.0241927.

[28] F. Bashir, W.-S. Baek, P. Sthapit, D. Pandey, and J.-Y. Pyun, "Coordinator assisted passive discovery for mobile end devices in IEEE 802.15. 4", in *Proc. of 2013 IEEE 10th Consumer Communications and Networking Conference (CCNC)*, 2013, pp. 601–604. DOI: 10.1109/CCNC.2013.6488506.

[29] H.-S. Ahn and W. Yu, "Environmental-adaptive RSSI-based indoor localization", *IEEE Transactions on Automation Science and Engineering*, vol. 6, no. 4, pp. 626–633, 2009. DOI: 10.1109/TASE.2008.2009126.

[30] B. M. Prakoso, A. Zainudin, P. Kristalina, and R. F. Azhar, "Performance evaluation of distribution node in case of LEACH implementation on wireless sensor network", *Journal Elektronika dan Telekomunikasi*, vol. 18, no. 2, pp. 67–74, 2018. DOI: 10.14203/jet.v18.67-74.

[31] M. A. Moridi, Y. Kawamura, M. Sharifzadeh, E. K. Chanda, M. Wagner, and H. Okawa, "Performance analysis of ZigBee network topologies for underground space monitoring and communication systems", *Tunnelling and Underground Space Technology*, vol. 71, pp. 201–209, 2018. DOI: 10.1016/j.tust.2017.08.018.

[32] F. Ding and A. Song, "Development and coverage evaluation of ZigBee-based wireless network applications", *J. Sensors*, vol. 2016, no. 1, pp. 1–9, 2016. DOI: 10.1155/2016/2943974.

[33] J. Schwinger, L. L. Deraad Jr., K. Milton, and W.-Y. Tsai, *Classical Electrodynamics*. CRC Press, 2019. DOI: 10.1201/9780429503542.